LETTER

doi:10.1038/nature11624

An ultraviolet-radiation-independent pathway to melanoma carcinogenesis in the red hair/fair skin background

Devarati Mitra[1], Xi Luo[2], Ann Morgan[1], Jin Wang[3], Mai P. Hoang[4], Jennifer Lo[1], Candace R. Guerrero[3], Jochen K. Lennerz[5], Martin C. Mihm[4], Jennifer A. Wargo[6], Kathleen C. Robinson[1], Suprabha P. Devi[1], Jillian C. Vanover[7], John A. D'Orazio[7], Martin McMahon[8], Marcus W. Bosenberg[9], Kevin M. Haigis[2], Daniel A. Haber[2], Yinsheng Wang[3] & David E. Fisher[1]

People with pale skin, red hair, freckles and an inability to tan—the 'red hair/fair skin' phenotype—are at highest risk of developing melanoma, compared to all other pigmentation types[1]. Genetically, this phenotype is frequently the product of inactivating polymorphisms in the melanocortin 1 receptor (*MC1R*) gene. *MC1R* encodes a cyclic AMP-stimulating G-protein-coupled receptor that controls pigment production. Minimal receptor activity, as in red hair/fair skin polymorphisms, produces the red/yellow pheomelanin pigment, whereas increasing MC1R activity stimulates the production of black/brown eumelanin[2]. Pheomelanin has weak shielding capacity against ultraviolet radiation relative to eumelanin, and has been shown to amplify ultraviolet-A-induced reactive oxygen species[3–5]. Several observations, however, complicate the assumption that melanoma risk is completely ultraviolet-radiation-dependent. For example, unlike non-melanoma skin cancers, melanoma is not restricted to sun-exposed skin and ultraviolet radiation signature mutations are infrequently oncogenic drivers[6]. Although linkage of melanoma risk to ultraviolet radiation exposure is beyond doubt, ultraviolet-radiation-independent events are likely to have a significant role[1,7]. Here we introduce a conditional, melanocyte-targeted allele of the most common melanoma oncoprotein, $BRAF^{V600E}$, into mice carrying an inactivating mutation in the *Mc1r* gene (these mice have a phenotype analogous to red hair/fair skin humans). We observed a high incidence of invasive melanomas without providing additional gene aberrations or ultraviolet radiation exposure. To investigate the mechanism of ultraviolet-radiation-independent carcinogenesis, we introduced an albino allele, which ablates all pigment production on the $Mc1r^{e/e}$ background. Selective absence of pheomelanin synthesis was protective against melanoma development. In addition, normal $Mc1r^{e/e}$ mouse skin was found to have significantly greater oxidative DNA and lipid damage than albino-$Mc1r^{e/e}$ mouse skin. These data suggest that the pheomelanin pigment pathway produces ultraviolet-radiation-independent carcinogenic contributions to melanomagenesis by a mechanism of oxidative damage. Although protection from ultraviolet radiation remains important, additional strategies may be required for optimal melanoma prevention.

To study the role of pigmentation in $BRAF^{V600E}$ melanoma development, we used a series of genetically matched mice on the C57BL/6 background with various pigmentation phenotypes (Fig. 1a). To mimic dark-skinned individuals with a high eumelanin-to-pheomelanin ratio, we used mice with the wild-type C57BL/6 pigmentation phenotype ('black'). To mimic individuals with the red hair/fair skin phenotype who carry a high pheomelanin-to-eumelanin ratio, we used mice with premature termination of the *Mc1r* transcript ($Mc1r^{e/e}$, 'red')[8]. To mimic individuals with albinism who have no melanin, we used mice with an inactivating mutation at the tyrosinase locus ($Tyr^{c/c}$, 'albino')[9]. Because tyrosinase is the initial and rate-limiting enzyme in melanin synthesis, albino melanocytes do not produce any pigment, but are normal in number and viability[10].

We generated two variants of each pigmentation phenotype. One variant contains melanocytes in the dermis. A second matched variant contains transgenic stem cell factor expressed under the keratin 14 promoter (*K14-SCF*), which mimics SCF expression in human epidermal keratinocytes and results in epidermal melanocyte localization[11].

To create a genetic context primed for the induction of melanoma we also introduced into each of our six variants a system for inducible, melanocyte-specific expression of oncogenic $BRAF^{V600E}$ (ref. 12). In humans, mice and zebrafish, expression of $BRAF^{V600E}$ in melanocytes primarily causes benign nevi, rather than melanoma[12–15]. In this context, malignant melanoma progression is thought to be constrained by

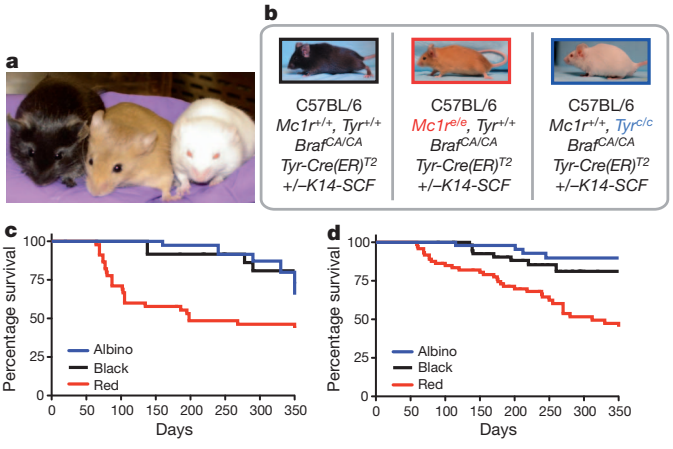

Figure 1 | Without ultraviolet radiation, $Braf^{CA}$ red mice have an increased rate of melanoma development relative to black and albino $Braf^{CA}$ animals. **a**, C57BL/6 pigmentation variants with epidermal melanocytes (*K14-SCF*). From left to right: black (wild type), red ($Mc1r^{e/e}$) and albino ($Tyr^{c/c}$). **b**, Genotype of animals used for experimental studies. **c**, Percentage survival of pigmentation variants not carrying the *K14-SCF* transgene, that is, no epidermal melanocytes ($n_{black} = 28$, $n_{red} = 40$, $n_{albino} = 48$). $P_{black–albino} = 0.250$, $P_{black–red} = 0.003$, $P_{albino–red} = 0.003$. **d**, Percentage survival of pigmentation variants carrying the *K14–SCF* transgene, that is, epidermal melanocytes ($n_{black} = 49$, $n_{red} = 77$, $n_{albino} = 41$). $P_{black–albino} = 0.103$, $P_{black–red} = 0.009$, $P_{albino–red} < 0.0001$.

[1]Cutaneous Biology Research Center, Massachusetts General Hospital, Charlestown, Massachusetts 02129, USA. [2]Massachusetts General Hospital Cancer Center, Charlestown, Massachusetts 02129, USA. [3]Department of Chemistry, University of California, Riverside, California 92521, USA. [4]Department of Pathology, Massachusetts General Hospital, Boston, Massachusetts 02114, USA. [5]Institute of Pathology, University Ulm, Ulm 89070, Germany. [6]Department of Surgery, Massachusetts General Hospital, Boston, Massachusetts 02114, USA. [7]Markey Cancer Center, University of Kentucky School of Medicine, Lexington, Kentucky 40536, USA. [8]Helen Diller Family Comprehensive Cancer Center, University of California San Francisco, San Francisco, California 94143, USA. [9]Department of Dermatology, Yale University School of Medicine, New Haven, Connecticut 06520, USA.

oncogene-induced senescence[15]. Consistent with this, expression of $BRAF^{V600E}$ in conjunction with silencing of *PTEN*, *TP53* or *CDKN2A* leads to development of malignant melanoma[12–14]. However, spontaneous progression of $BRAF^{V600E}$-expressing melanocytes to malignant melanoma has been reported following a long latency period in C57BL/6 mice, although this phenomenon was not seen on an outbred model[12,16,17].

We initially produced six groups of $BRAF^{V600E}$ inducible ('$Braf^{CA}$') mice representing three pigmentation variants ('black', 'red' and 'albino') with or without epidermal melanocytes (+/− *K14-SCF*, Fig. 1b). Melanocyte-selective expression of $BRAF^{V600E}$ was achieved by tamoxifen-mediated activation of Cre recombinase (*Tyr-Cre(ER)*^{T2}) in adult mice carrying the $Braf^{CA}$ allele. The animals were then followed without environmental genotoxic stressors (such as ultraviolet radiation). Black and albino $Braf^{CA}$ mice developed similarly low rates of melanoma after a long latency (regardless of *K14-SCF* status). In contrast, red $Braf^{CA}$ mice developed melanomas at an accelerated rate with >50% having tumours after 1 year, regardless of *K14-SCF* status (Fig. 1c, d).

The tumours on the black, red and albino backgrounds were grossly amelanotic and largely on the dorsal trunk (within the tamoxifen-treated areas). Occasionally, a tumour would develop on the ventral trunk, tail or paw, which may reflect a predictable spread of tamoxifen secondary to grooming. (Fig. 2a–c). The tumours, which were primarily dermal, were generally amelanotic on the red and albino backgrounds, whereas the melanomas in black mice often had superficial pigmentation adjacent to the epidermis (Fig. 2d–f). Regardless of pigmentation background, the tumours were histologically similar with spindle cell features which were not easily distinguishable from tumours on C57BL/6 $Braf^{CA}$-$Pten^{flox/flox}$ animals generated in parallel (compare Fig. 2 with Supplementary Fig. 1). On closer examination, occasional red-$BRAF^{V600E}$ tumour cells were found to contain melanin (Fig. 2g, h). It was further possible to increase pigmentation in the most superficial melanoma cells with topical application of forskolin, an adenylate cyclase agonist known to stimulate skin pigmentation[18] (Fig. 2i). The limited induction of pigmentation is likely related to the poor tissue penetration of forskolin, but nonetheless demonstrates the ability of the melanoma cells to become hyper-pigmented *in vivo* upon activation of cAMP signalling.

Tumours on all three pigmentation backgrounds stained positively for S100, a standard immunohistochemical melanoma marker (Fig. 2j). In addition, reverse transcriptase polymerase chain reaction (RT–PCR) showed that the tumours consistently express the melanocytic pigment genes *M-Mitf*, *Dct*, *Tyrp1* and *Tyr* (Fig. 3a, d and data not shown). In addition, occasional $HMB45^{+}$ cells could be found by immunofluorescence (Supplementary Fig. 2). The tumours on all three pigmentation backgrounds were locally invasive to fat and skeletal muscle with active mitoses. Although no gross visceral organ metastases were observed, small clusters of cells expressing gp100, the premelanosome-associated glycoprotein (Pmel/gp100/HMB45), could be found in skin draining lymph nodes (Fig. 2k).

Using a primary cell line derived from one of the red mouse melanomas, we observed that forskolin upregulated the expression of the melanocyte-specific isoform of *Mitf* (*M-Mitf*), and produced a marked increase in expression of the *Dct* and *Tyrp1* pigment genes, consistent with the ability of the cells to respond to melanocytic differentiation signals (Fig. 3a).

To determine whether the melanoma cells were dependent on the presumed oncogenic driver $BRAF^{V600E}$, we tested their response to small molecule inhibitors of BRAF or MEK (also known as MAP2K). Treatment with the oncogenic BRAF inhibitor, PLX4720, or the MEK inhibitor, U0126, prevented melanoma cell proliferation *in vitro*, and PLX4720 blocked tumour cell growth *in vivo*, consistent with a dependency of these tumours on the $BRAF^{V600E}$ oncoprotein (Fig. 3b, c). BRAF inhibition also elevated the expression of melanocytic genes as previously reported in human melanomas (Fig. 3d)[19].

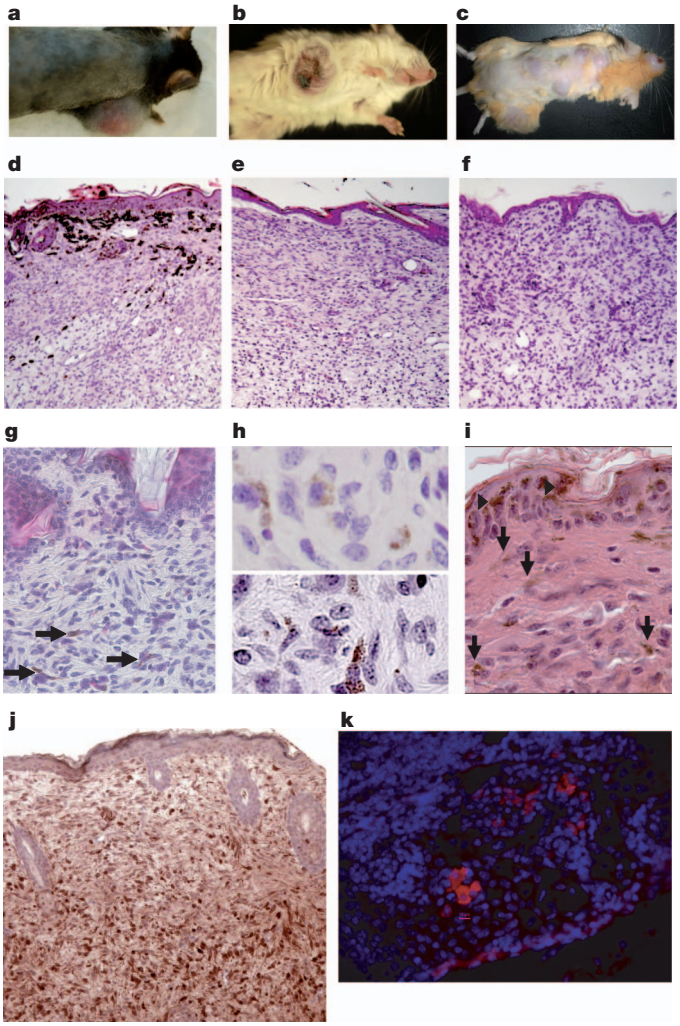

Figure 2 | Melanomas on all three pigmentation variants are morphologically similar and exhibit common histologic features. **a**–**c**, Melanomas on black (**a**), albino (**b**) and red (**c**) mice are grossly amelanotic. **d**–**f**, Histologically, black (**d**), albino (**e**) and red (**f**) melanomas are also mostly amelanotic, although superficial tumour cells in black-$BRAF^{V600E}$ tumours carry melanin (original magnification, ×10). **g**, Red-$BRAF^{V600E}$ melanomas can also carry pigment (arrows) (original magnification, ×20). **h**, Further magnification of two red melanomas also illustrates pigmented tumour cells (original magnification, ×100). **i**, Forskolin induces epidermal pigmentation (arrowheads) and mild tumour cell pigmentation (arrows) (original magnification, ×20). **j**, Tumour cells stain positive for S100 (original magnification, ×10). **k**, Skin-draining lymph nodes carry $gp100^{+}$ cells (red) (scale bar, 10 μm).

Because inactivating mutations in *Mc1r* alter cAMP levels in the cell, red mice undoubtedly have numerous intracellular pathway differences relative to wild-type $Mc1r^{E/E}$ (black) animals, including altered DNA repair[20]. We therefore wished to study whether the pheomelanin pigment pathway itself has an intrinsic mechanistic role, or whether it is merely a marker of melanoma risk. To investigate this question we introduced the albino tyrosinase ($Tyr^{c/c}$) allele into the red $Mc1r^{e/e}$ background to test melanoma incidence in albino-$Mc1r^{e/e}$ animals, which retain low MC1R activity and also lack all pigment production (Fig. 4a). A melanocyte-targeted *LacZ* transgene was used to confirm that the albino allele does not alter melanocyte number in these mice (Supplementary Fig. 3a, b)[10]. As shown in Fig. 4b, the albino allele profoundly protected red mice from melanoma. The rare albino-$Mc1r^{e/e}$ melanomas occurred after long latency and had the same amelanotic, $S100^{+}$, histologic features as the other pigmentation variant $Braf^{CA}$ animals (Supplementary Fig. 4a–c). This observation suggests

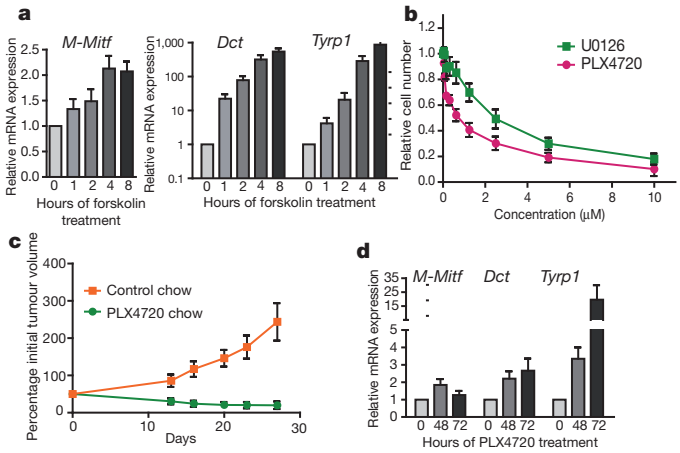

Figure 3 | Tumour cells from a red-*Braf*^{CA} animal behave like classic BRAF^{V600E} melanomas after cAMP upregulation or BRAF inhibition. **a**, Forskolin (20 μM) upregulates expression of melanocytic markers ($n = 4$). **b**, MAPK inhibition by PLX4720 or U0126 decreases melanoma cell proliferation ($n = 3$). **c**, PLX4720 blocks melanoma growth *in vivo* ($n = 3$). **d**, PLX4720 (2 μM) upregulates expression of melanocytic markers. Relative mRNA expression normalized to 18S ribosomal RNA and 0 h time point. Error bars denote s.e.m.

that the pheomelanin synthesis pathway is necessary for the high rate of ultraviolet-radiation-independent melanoma in the red mice.

Previous studies have demonstrated that ultraviolet radiation amplifies reactive oxygen species (ROS) production and subsequent oxidative DNA damage in the skin of pigmented mice[21]. Cells with high pheomelanin levels that receive ultraviolet radiation have been found to carry particularly high levels of oxidative damage[4,5]. Because darkly pigmented individuals carry both pheomelanin and eumelanin, it has been proposed that their lower melanoma risk may result from eumelanin intermediates and polymers absorbing ROS and functioning as *in vivo* antioxidants[22,23].

To determine whether ROS-mediated oxidative DNA damage is affected by the pheomelanin synthesis pathway, levels of 8,5′-cyclo-2′-deoxyadenosine (cdA) and 8,5′-cyclo-2′-deoxyguanosine (cdG) were measured in DNA isolated from skin of red-*Mc1r*$^{e/e}$ and albino-*Mc1r*$^{e/e}$ mice, using a previously reported liquid chromatography-tandem mass spectrometric method[24] (Fig. 4c). These two ROS-mediated cyclopurines are unlikely to be artificially induced during sample preparation and are quite stable[25,26]. Significantly, replication studies in *Escherichia coli* have shown that *S*-cdA and *S*-cdG can lead to A-to-T and G-to-A mutations at frequencies of 11% and 20%, respectively[27]. Comparing cyclopurine levels in the skin of various pigmentation-variant mice, it was found that the levels of cdA and cdG are significantly higher in skin from red-*Mc1r*$^{e/e}$ mice compared to skin from albino-*Mc1r*$^{e/e}$ animals (Fig. 4d, e). This observation indicates that activation of the pheomelanin synthesis pathway results in increased oxidative DNA damage. Correlative evidence for increased cellular oxidative stress was also found in the observation that red-*Mc1r*$^{e/e}$ mouse skin carries higher levels of lipid peroxides, a product of ROS-mediated lipid damage (Fig. 4f).

The findings reported here indicate that in the context of oncogenic BRAF activation, individuals carrying red hair/fair skin *MC1R* polymorphisms have an increased risk of melanoma, owing to both poor

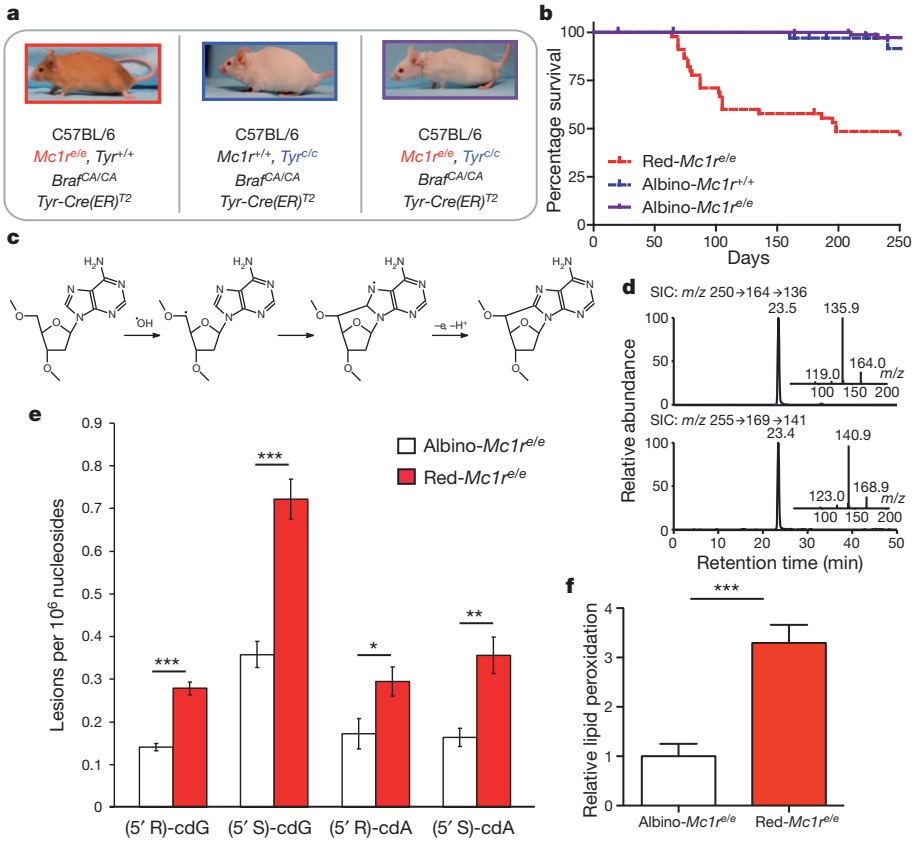

Figure 4 | The ultraviolet-radiation-independent propensity of red *Braf*^{CA} mice to develop melanoma is dependent on pigment production. **a**, Genotypes of mice studied. **b**, The albino allele protects *Mc1r*$^{e/e}$ mice from melanoma development ($n_{red} = 40$, $n_{albino} = 48$, $n_{albino\text{-}red} = 90$) $P_{albino\text{–}albino\text{-}red} = 0.308$, $P_{albino\text{–}red} < 0.0001$, $P_{red\text{–}albino\text{-}red} < 0.0001$. **c**, ROS react with purine nucleosides to produce 8,5′-cyclopurine lesions (cdA shown). **d**, Selected-ion chromatograms for DNA from albino-*Mc1r*$^{e/e}$ mouse skin. The insets show the positive-ion MS/MS/MS spectra for unlabelled and labelled *S*-cdA. **e**, Both diastereomers of cdA and cdG are significantly higher in red-*Mc1r*$^{e/e}$ skin ($n = 3$). $^*P < 0.05$; $^{**}P < 0.01$; $^{***}P < 0.001$. **f**, Lipid peroxide levels are significantly higher in red-*Mc1r*$^{e/e}$ skin ($n = 3$), $^{***}P < 0.0001$.

protection from environmental carcinogens like ultraviolet radiation, and also via intrinsic carcinogenic features of pheomelanin synthesis; potentially via pheomelanin itself, an intermediate of pigment synthesis or a by-product of the pathway.

In humans, there are multiple *MC1R* polymorphisms with varied perturbation of receptor function that produce a red hair/fair skin phenotype; however, a unifying feature of these various polymorphisms is a high pheomelanin-to-eumelanin ratio, which is also produced by the $Mc1r^{e/e}$ allele in mice. Recent data intriguingly demonstrated that black animals overexpressing hepatocyte growth factor (HGF) who receive ultraviolet radiation are at a higher risk of melanoma than their albino counterparts[21]. Although the present study reveals a small difference between black and albino $BRAF^{V600E}$-driven melanomas in the presence of *K14-SCF* (Fig. 1d), the effect did not reach statistical significance ($P = 0.103$), perhaps signifying oncogene-specific differences. It seems that the effects of pigmentation and ultraviolet radiation are likely to work together in determining melanoma risk.

The photometer used for our laboratory's routine calibration (International Light 1400) was unable to detect any measurable ultraviolet radiation in our mouse cages during ambient light exposure. However, strong epidemiological work links ultraviolet radiation to melanoma, and the current data do not diminish the importance of sun exposure as a key contributing factor[1]. In humans, it is likely that the ultraviolet-independent effects act in concert with ultraviolet-mediated cellular toxicity. In agreement with published studies, ultraviolet radiation at a UV-A/UV-B ratio similar to that found in sunlight (10 J cm^{-2} UV-A and 0.65 J cm^{-2} UV-B) was found to exacerbate oxidative damage selectively in red mouse skin as measured by levels of lipid peroxidation[4,5] (Supplementary Fig. 5a). Studies are underway to investigate whether ultraviolet radiation is able to alter the red-$BRAF^{V600E}$ tumour phenotype. Preliminary studies examining the effect of visible light (180 J cm^{-2}) did not reveal significantly altered lipid peroxidation in any pigmentation context ($P = 0.4506$). Perhaps, however, there is a trend towards an increased level of lipid peroxidation in red mouse skin (Supplementary Fig. 5b).

Further evidence suggesting an ultraviolet-radiation-independent red hair/fair skin melanoma risk is the observation that although darker-skinned individuals have a significantly lower risk of melanoma than lighter-skinned individuals, the sun protective factor (SPF, a measurement of sunburn protection) of darker skin has been estimated at only in the range of SPF 2.0–4.0 (ref. 28). In addition, sunscreen (typically SPF 20–40) has shown weak efficacy in protecting against melanoma, unlike its protection against cutaneous squamous cell carcinoma[29,30]. There are numerous potential explanations for the sunscreen-melanoma data including the possibility that ultraviolet radiation shielding may protect against only one of several carcinogenic mechanisms—with the intrinsic pheomelanin pathway representing an additional contributor to melanomagenesis via ultraviolet-radiation-independent means. These data are not evidence against a role for ultraviolet radiation in melanomagenesis. Indeed, the effect of ultraviolet radiation is likely to exacerbate this mechanism, such that ultraviolet radiation shielding and sunscreen remain extremely important for skin cancer prevention. However, further preventative strategies may be essential to optimally diminish melanoma risk in the most susceptible individuals.

METHODS SUMMARY

Mice. At 6–10 weeks of age, mice were treated topically with 20 mg ml^{-1} tamoxifen for 5 days. For topical darkening, 20% coleus extract was applied as previously described[17]. For *in vivo* PLX4720 studies, animals were given *ad libitum* mouse chow containing 2% PLX4720 by weight. All studies and procedures involving animal subjects were approved by the Institutional Animal Care and Use Committees of Massachusetts General Hospital and Dana-Farber Harvard Cancer Center, and were conducted strictly in accordance with the approved animal handling protocol.

Morphological examination. Histology and immunostaining were performed according to established protocols using anti-S100 (Dako), anti-DCT (Santa Cruz), anti-C5 MITF (tissue culture supernatant), anti-HMB45 (Santa Cruz) and anti-gp100 (Abcam) antibodies.

Primary cell culture. Primary tumour was digested overnight and grown in DMEM. Proliferation was measured by the CellTiter-Glo Luminescent Cell Viability Assay (Promega).

Quantitative RT–PCR. Messenger RNA expression of melanocytic markers was determined using intron-spanning mouse-specific primers with SYBR FAST qPCR master mix (Kapa Biosystems).

Measurement of 8,5′-cyclopurine-2′-deoxynucleosides. cdA and cdG levels were measured as previously published[24]. Briefly, nuclear DNA was isolated from mouse skin, digested to nucleosides, separated by high-performance liquid chromatography (HPLC) and analysed by liquid chromatography–multi-stage mass spectrometry (LC–MS/MS/MS).

Measurement of lipid peroxidation. Mouse skin was irradiated with ultraviolet (10 J cm^{-2} UV-A and 0.65 J cm^{-2} UV-B), or visible light (180 J cm^{-2}). After homogenization, lipid peroxidation was measured with the OxiSelect TBARS Assay Kit (Cell Biolabs).

Full Methods and any associated references are available in the online version of the paper.

Received 27 February; accepted 27 September 2012.
Published online 31 October 2012.

1. Rhodes, A. R., Weinstock, M. A., Fitzpatrick, T. B., Mihm, M. C. J. & Sober, A. J. Risk factors for cutaneous melanoma. A practical method of recognizing predisposed individuals. *J. Am. Med. Assoc.* **258,** 3146–3154 (1987).
2. Valverde, P., Healy, E., Jackson, I., Rees, J. L. & Thody, A. J. Variants of the melanocyte-stimulating hormone receptor gene are associated with red hair and fair skin in humans. *Nature Genet.* **11,** 328–330 (1995).
3. Rouzaud, F., Kadekaro, A. L., Abdel-Malek, Z. A. & Hearing, V. J. MC1R and the response of melanocytes to ultraviolet radiation. *Mutat. Res.* **571,** 133–152 (2005).
4. Wenczl, E. *et al.* (Pheo)melanin photosensitizes UVA-induced DNA damage in cultured human melanocytes. *J. Invest. Dermatol.* **111,** 678–682 (1998).
5. Hill, H. Z. & Hill, G. J. UVA, pheomelanin and the carcinogenesis of melanoma. *Pigment Cell Res.* **13** (suppl. 8), 140–144 (2000).
6. Curtin, J. A. *et al.* Distinct sets of genetic alterations in melanoma. *N. Engl. J. Med.* **353,** 2135–2147 (2005).
7. Elwood, J. M. & Jopson, J. Melanoma and sun exposure: an overview of published studies. *Int. J. Cancer* **73,** 198–203 (1997).
8. Robbins, L. S. *et al.* Pigmentation phenotypes of variant extension locus alleles result from point mutations that alter MSH receptor function. *Cell* **72,** 827–834 (1993).
9. Halaban, R. *et al.* Tyrosinases of murine melanocytes with mutations at the albino locus. *Proc. Natl Acad. Sci. USA* **85,** 7241–7245 (1988).
10. Vanover, J. C. *et al.* Stem cell factor rescues tyrosinase expression and pigmentation in discreet anatomic locations in albino mice. *Pigment Cell Melanoma Res.* **22,** 827–838 (2009).
11. Kunisada, T. *et al.* Murine cutaneous mastocytosis and epidermal melanocytosis induced by keratinocyte expression of transgenic stem cell factor. *J. Exp. Med.* **187,** 1565–1573 (1998).
12. Dankort, D. *et al.* $Braf^{V600E}$ cooperates with *Pten* loss to induce metastatic melanoma. *Nature Genet.* **41,** 544–552 (2009).
13. Patton, E. E. *et al.* BRAF mutations are sufficient to promote nevi formation and cooperate with p53 in the genesis of melanoma. *Curr. Biol.* **15,** 249–254 (2005).
14. Goel, V. K. *et al.* Melanocytic nevus-like hyperplasia and melanoma in transgenic BRAFV600E mice. *Oncogene* **28,** 2289–2298 (2009).
15. Michaloglou, C. *et al.* $BRAF^{E600}$-associated senescence-like cell cycle arrest of human naevi. *Nature* **436,** 720–724 (2005).
16. Dhomen, N. *et al.* Oncogenic Braf induces melanocyte senescence and melanoma in mice. *Cancer Cell* **15,** 294–303 (2009).
17. Rae, J. *et al.* *^{V600E}Braf::Tyr-CreERT2::K14-Kitl* mice do not develop superficial spreading-like melanoma: keratinocyte kit ligand is insufficient to "translocate" ^{V600E}Braf-driven melanoma to the epidermis. *J. Invest. Dermatol.* **132,** 488–491 (2012).
18. D'Orazio, J. A. *et al.* Topical drug rescue strategy and skin protection based on the role of *Mc1r* in UV-induced tanning. *Nature* **443,** 340–344 (2006).
19. Boni, A. *et al.* Selective $BRAF^{V600E}$ inhibition enhances T-cell recognition of melanoma without affecting lymphocyte function. *Cancer Res.* **70,** 5213–5219 (2010).
20. Kadekaro, A. L. *et al.* Melanocortin 1 receptor genotype: an important determinant of the damage response of melanocytes to ultraviolet radiation. *FASEB J.* **24,** 3850–3860 (2010).
21. Noonan, F. P. *et al.* Melanoma induction by ultraviolet A but not ultraviolet B radiation requires melanin pigment. *Nature Commun.* **3,** 884 (2012).
22. Nofsinger, J. B., Liu, Y. & Simon, J. D. Aggregation of eumelanin mitigates photogeneration of reactive oxygen species. *Free Radic. Biol. Med.* **32,** 720–730 (2002).
23. Kovacs, D. *et al.* The eumelanin intermediate 5,6-dihydroxyindole-2-carboxylic acid is a messenger in the cross-talk among epidermal cells. *J. Invest. Dermatol.* **132,** 1196–1205 (2012).
24. Wang, J. *et al.* Quantification of oxidative DNA lesions in tissues of Long-Evans Cinnamon rats by capillary high-performance liquid chromatography–tandem mass spectrometry coupled with stable isotope-dilution method. *Anal. Chem.* **83,** 2201–2209 (2011).

25. Wang, Y. Bulky DNA lesions induced by reactive oxygen species. *Chem. Res. Toxicol.* **21,** 276–281 (2008).
26. Jaruga, P. & Dizdaroglu, M. 8,5′-Cyclopurine-2′-deoxynucleosides in DNA: mechanisms of formation, measurement, repair and biological effects. *DNA Repair (Amst.)* **7,** 1413–1425 (2008).
27. Yuan, B., Wang, J., Cao, H., Sun, R. & Wang, Y. High-throughput analysis of the mutagenic and cytotoxic properties of DNA lesions by next-generation sequencing. *Nucleic Acids Res.* **39,** 5945–5954 (2011).
28. Neugut, A. I., Kizelnik-Freilich, S. & Ackerman, C. Black-white differences in risk for cutaneous, ocular, and visceral melanomas. *Am. J. Public Health* **84,** 1828–1829 (1994).
29. Green, A. C., Williams, G. M., Logan, V. & Strutton, G. M. Reduced melanoma after regular sunscreen use: randomized trial follow-up. *J. Clin. Oncol.* **29,** 257–263 (2011).
30. Huncharek, M. & Kupelnick, B. Use of topical sunscreens and the risk of malignant melanoma: a meta-analysis of 9067 patients from 11 case-control studies. *Am. J. Public Health* **92,** 1173–1177 (2002).

Supplementary Information is available in the online version of the paper.

Acknowledgements We thank T. Kunisada for generously sharing *K14-SCF* mice and C. L. Evans for help with mouse skin irradiation. We also thank A. P. Codgill for help with primary tumour cell culture and A. Piris for pathology consultation as well as M. Haigis and Z. Abdel-Malik for discussions. This work was supported by the following grants from the National Institutes of Health 5R01 AR043369-16 (D.E.F.), R01-CA101864 (Y.W.) and F30 ES020663-01 (D.M.), as well as support from the Dr Miriam and Sheldon G. Adelson Medical Research Foundation, the US-Israel Binational Science Foundation, and the Melanoma Research Alliance (D.E.F.).

Author Contributions D.M. and D.E.F. conceived and planned the project. M.M., M.W.B. and K.M.H. provided the mice carrying the *PTEN*, $BRAF^{V600E}$ and $Tyr\text{-}Cre(ER)^{T2}$ alleles. D.M. performed the mouse work with help from A.M., J.L., S.P.D. and K.C.R. Histology was performed by D.M., X.L., J.C.V. and J.A.D. with support from D.A.H. Pathological analysis was provided by M.P.H., J.K.L. and M.C.M. *In vitro* studies were performed by D.M. with help from A.M. and J.L. J.A.W. generated the primary mouse cell line. J.W., C.R.G. and Y.W. collected DNA from mouse skin and performed LC–MS/MS/MS. The manuscript was written by D.M. and D.E.F. All authors discussed the results and commented on the manuscript.

Author Information Reprints and permissions information is available at www.nature.com/reprints. The authors declare no competing financial interests. Readers are welcome to comment on the online version of the paper. Correspondence and requests for materials should be addressed to D.E.F. (dfisher3@partners.org).

METHODS

Mice. All animals used for breeding were backcrossed a minimum of six generations onto the C57BL/6 genetic background (this corresponds to a >98.4% C57BL/6 congenic animal, http://jaxmice.jax.org/support/nomenclature/tutorial.html). The black (wild type), red ($Mc1r^{e/e}$) and albino ($Tyr^{c/c}$) animals were purchased from Jackson Laboratories. *K14-SCF* animals were acquired from T. Kunisada. Genotyping of each litter, including the $Tyr\text{-}Cre(ER)^{T2}$, $Braf^{CA}$ and $PTEN^{flox/flox}$ alleles was performed as previously published[10,11]. At 6–10 weeks of age the dorsal fur was trimmed using animal shears with a 0.25 mm head and the mice were treated topically with 20 mg ml^{-1} tamoxifen for 5 consecutive days. For tumour darkening, a 20% solution of *Coleus forskohlii* root extract (80 μM forskolin) was topically applied daily as previously described[17]. For *in vivo* PLX4720 studies, animals were given *ad libitum* mouse chow containing 2% PLX4720 by weight or control chow acquired from Plexxikon. All studies and procedures involving animal subjects were approved by the Institutional Animal Care and Use Committees of Massachusetts General Hospital and Dana-Farber Harvard Cancer Center and were conducted strictly in accordance with the approved animal handling protocol.

Dissection and histology. Tissues of interest were photographed, excised, weighed, rinsed in PBS, fixed in 10% neutral-buffered formalin, rinsed in PBS, and stored in 70% ethanol. Formalin-fixed tissues were paraffin embedded (FFPE) and sectioned (3–5 μm) using standard procedures. Morphological analysis was performed using multiple independent samples per site/organ (5 to 9 samples per genotype) as well as >6 animals. Two pathologists (J.K.L., M.P.H.) independently examined the histopathology of the tumour samples. Digitization and image capture was performed using an Olympus DP70 digital camera (Olympus) connected to an Olympus BX51 light microscope or a Scanscope whole-slide scanning system (Aperio).

Immunohistochemistry. For immunohistochemistry, sections were deparaffinized with xylene and hydrated with a graded series of alcohol. Sections were boiled in 50 mM Tris-buffer (pH 9) or citrate for antigen retrieval and rinsed in PBS. Sections were blocked in 1% BSA, 0.1% Triton X-100 PBS, incubated with 1:200 dilutions of rabbit anti-S100 (Dako), 1:100 dilutions of goat anti-DCT (Santa Cruz), 1:200 dilutions of mouse anti-HMB45 (Santa Cruz) and 1:200 dilutions of mouse anti-gp100 (Abcam) antibodies, followed by visualization with appropriate secondary antibodies conjugated to Alexa594 or Alexa488 (1:500). Appropriate controls for specificity of staining were included and images were captured using an upright fluorescence microscope (Eclipse 90i, Nikon). To identify epidermal melanocytes, skin from reporter mice carrying the various pigmentation alleles and the *K14-SCF* transgene as well as a *DCT-LacZ* reporter allele was cryosectioned and stained with 5-bromo-4-chloro-3-indolyl-β-D-galactoside (X-gal) and nuclear fast red counterstaining.

Primary cell culture. Tumour cells were digested overnight in 10 mg ml^{-1} collagenase and 1 mg ml^{-1} hyaluronidase. Initially tumour cells were grown in RPMI media with HEPES and 20% serum. Subsequently tumour cells were grown in DMEM media with 10% serum. Proliferation after 72 h of PLX4720 (Chemietek) and U0126 (Cell Signaling) was determined by the CellTiter-Glo Luminescent Cell Viability Assay (Promega).

Quantitative RT–PCR. RNA was collected from primary cultured tumour cells treated for varying times with forskolin or PLX4720 using the RNeasy Plus mini kit (Qiagen). mRNA expression of melanocytic markers was determined using intron-spanning mouse-specific primers with Kapa SYBR FAST qPCR master mix (Kapa Biosystems). Expression was normalized to 18S rRNA and 0 h time points. Primer sequences used: *Mitf* forward GCCTGAAACCTTGCTATGC TGGAA, *Mitf* reverse AAGGTACTGCTTTACCTGGTGCCT, *Dct* forward AGGTACCATCTGTTGTGGCTGGAA, *Dct* reverse AGTTCCGACTAATCA GCGTTGGGT, *Tyrp1* forward TGGGGATGTGGATTTCTCTC, *Tyrp1* reverse AGGGAGAAAGAAGGCTCCTG, *18S* forward AGGTTCTGGCCAACGG TCTAG, *18S* reverse CCCTCTATGGGCAATTTT.

Extraction of nuclear DNA from mouse skin tissues. Nuclear DNA was isolated from mouse skin using a high-salt method. Tissues were ground under liquid nitrogen into fine powder using a mortar and pestle. A nuclei lysis buffer containing 20 mM Tris (pH 8.3), 20 mM EDTA, 400 mM NaCl, 1% SDS (w/v) and 0.05% proteinase K (w/v) was added to the tissue and incubated in a water bath at 55 °C overnight. Half volume of saturated NaCl solution was added to the digestion mixture, incubated at 55 °C for 15 min then centrifuged at ~12,000*g* for 30 min. The supernatant was collected and centrifuged again. The nucleic acids in the supernatant were precipitated with cold ethanol, dissolved in water and incubated in the presence of 0.03% RNase A (w/v) and 0.25 U μl^{-1} of RNase T1 at 37 °C overnight, and subsequently extracted with an equal volume of chloroform/isoamyl alcohol (24:1, v/v) twice. The DNA was then precipitated from the aqueous layer by cold ethanol, centrifuged at 10,000*g* at 4 °C for 15 min, washed twice with 70% cold ethanol and dried under vacuum. The DNA pellet was dissolved in deionized water and quantified by using ultraviolet absorption spectrophotometry.

Enzymatic digestion of nuclear DNA. Nuclease P1 (16 U), phosphodiesterase 2 (0.025 U), 20 nmol of erythro-9-(2-hydroxy-3-nonyl) adenine (EHNA) and a 30 μl solution containing 300 mM sodium acetate (pH 5.6) and 10 mM zinc chloride were added to 200 μg of DNA. In this context, EHNA served as an inhibitor for deamination of 2′-deoxyadenosine to 2′-deoxyinosine (dI) induced by adenine deaminase. The above digestion was continued at 37 °C for 48 h. To the digestion mixture were then added alkaline phosphatase (10 U), phosphodiesterase 1 (0.0125 U) and 60 μl of 0.5 M Tris-HCl buffer (pH 8.9). The digestion was continued at 37 °C for 2 h and subsequently neutralized by addition of formic acid. To the mixture were then added uniformly ^{15}N-labelled standard lesions, which included 400 fmol of *R*-cdG, 150 fmol of *S*-cdG, 80 fmol of *R*-cdA and 40 fmol of *S*-cdA. The enzymes in the digestion mixture were subsequently removed by chloroform extraction twice. The resulting aqueous layer was subjected to off-line high-performance liquid chromatography (HPLC) separation for the enrichment of the lesions under study, following our previously described procedures[26].

Liquid chromatography–multi-stage mass spectrometry (LC–MS/MS/MS) analysis. The LC–MS/MS/MS experiments were conducted using an LTQ linear ion trap mass spectrometer using our recently described conditions[26]. Briefly, the amounts of cdA and cdG lesions in each nucleoside sample were calculated based on the ratios of peak areas found in the selected-ion chromatograms for the analyte (for example, the 23.5 min peak in the top panel of Fig. 4d for *S*-cdA) and the corresponding stable isotope-labelled standard (for example, the 23.4 min peak in the bottom panel of Fig. 4d for the ^{15}N-labelled *S*-cdA), the known amount of uniformly ^{15}N-labelled standard was added to the nucleoside mixture (for example, 40 fmol for *S*-cdA), and calibration curves. The calibration curves were constructed from the same LC–MS/MS/MS analyses of a series of mixtures with known compositions of the unlabelled cdA, cdG and constant amounts of the corresponding uniformly ^{15}N-labelled standards, as described previously[26]. The lesion formation frequencies as shown in Fig. 4e were then calculated by dividing the amounts of cdA and cdG in the sample with the total amount of nucleosides present.

Skin irradiation and lipid peroxide measurement. Six-week-old mice were euthanized and fur was removed using animal shears with a 0.25 mm head. Twelve sections of skin, each with an area of 1 cm^2, were removed from each mouse and placed in 35-mm dishes on ice after adherence to Whatman filter paper suspended in PBS. For each ultraviolet and visible light study, six sections of skin from each mouse were placed in the dark on ice as controls. For ultraviolet studies, six sections of skin from each mouse were irradiated on ice with 10 J cm^{-2} UV-A and 0.65 J cm^{-2} UV-B at an irradiance of 6.67 mW cm^{-2} using a Sylvania 350 Blacklight (Osram Sylvania). This ultraviolet distribution is comparable to natural sunlight (96.65% UV-A and 3.35% UV-B). Two mice of each pigmentation type were used for a total of $n = 12$ skin samples for each condition. For visible light studies, six sections of skin from each mouse were irradiated on ice with 180 J cm^{-2} visible light from a Dolan-Jenner A3200 Fiber-Lite Illuminator at an irradiance of 200 mW cm^{-2}. The illuminator bulb was fit with a Thorlabs FEL0400 Edgepass ultraviolet filter with a transmission of <0.001% for wavelengths <400 nm, such that no irradiation output was detectable in the ultraviolet range below 400 nm. One mouse of each pigmentation type was used for a total of six skin samples for each condition. Following treatment, skin sections were flash-frozen and homogenized in PBS containing the antioxidant butylated hydroxytoluene (BHT) to prevent further lipid peroxidation, using a Qiagen TissueLyser II. Homogenized samples were centrifuged and supernatants were collected. Protein content of each sample was determined by Coomassie Plus Protein Assay, and samples were diluted with PBS plus BHT for normalization of sample concentration (Thermo Scientific). Lipid peroxidation of each irradiated set of sample was determined using an OxiSelect TBARS Assay kit and normalized to its unirradiated control (Cell Biolabs).